Cell Metabolism
Article

Endocrine Regulation of the Fasting Response by PPARα-Mediated Induction of Fibroblast Growth Factor 21

Takeshi Inagaki,[1] Paul Dutchak,[1] Guixiang Zhao,[1] Xunshan Ding,[2,3] Laurent Gautron,[2,4,5] Vinay Parameswara,[4] Yong Li,[8] Regina Goetz,[9] Moosa Mohammadi,[9] Victoria Esser,[4] Joel K. Elmquist,[2,4,5] Robert D. Gerard,[1,4] Shawn C. Burgess,[6] Robert E. Hammer,[7] David J. Mangelsdorf,[2,3] and Steven A. Kliewer[1,2,*]
[1] Department of Molecular Biology
[2] Department of Pharmacology
[3] Howard Hughes Medical Institute
[4] Department of Internal Medicine
[5] Division of Hypothalamic Research
[6] Advanced Imaging Research Center
[7] Department of Biochemistry
University of Texas Southwestern Medical Center, Dallas, TX 75390, USA
[8] Van Andel Research Institute, Grand Rapids, MI 49503, USA
[9] Department of Pharmacology, New York University School of Medicine, New York, NY 10016, USA
*Correspondence: steven.kliewer@utsouthwestern.edu
DOI 10.1016/j.cmet.2007.05.003

SUMMARY

Peroxisome proliferator-activated receptor α (PPARα) regulates the utilization of fat as an energy source during starvation and is the molecular target for the fibrate dyslipidemia drugs. Here, we identify the endocrine hormone fibroblast growth factor 21 (FGF21) as a mediator of the pleiotropic actions of PPARα. *FGF21* is induced directly by PPARα in liver in response to fasting and PPARα agonists. FGF21 in turn stimulates lipolysis in white adipose tissue and ketogenesis in liver. FGF21 also reduces physical activity and promotes torpor, a short-term hibernation-like state of regulated hypothermia that conserves energy. These findings demonstrate an unexpected role for the PPARα-FGF21 endocrine signaling pathway in regulating diverse metabolic and behavioral aspects of the adaptive response to starvation.

INTRODUCTION

Mammals have evolved complex metabolic and behavioral responses to survive extended periods of nutrient deprivation. A key aspect of the overall adaptive response is the shift from carbohydrates to ketone bodies as a primary fuel source. During fasting and starvation, fatty acids are mobilized from white adipose tissue (WAT) to liver, where they are oxidized to acetyl-CoA. The acetyl-CoA is then used to synthesize ketone bodies, including β-hydroxybutyrate and acetoacetate, which are reconverted to acetyl-CoA in other tissues and oxidized in the tricarboxylic acid cycle to produce energy (Fukao et al., 2004). During prolonged fasts, ketone bodies provide nearly half of the body's total energy and up to 70% of the energy required by the brain (Cahill, 2006). In addition to altering their fuel sources, many small mammals conserve energy when food is scarce by undergoing periodic bouts of torpor, a hibernation-like state of regulated hypothermia generally lasting several hours (Geiser, 2004).

Peroxisome proliferator-activated receptor α (PPARα), a nuclear receptor activated by fatty acids, is required for the normal adaptive response to starvation. PPARα binds to DNA response elements as a heterodimer with the retinoid X receptor (RXR) to regulate the transcription of numerous genes involved in fatty acid transport and oxidation (Kersten et al., 2000; Lefebvre et al., 2006). Among the genes regulated directly by PPARα in liver are those encoding acyl-CoA oxidase (ACOX1) (Tugwood et al., 1992), which is involved in peroxisomal β-oxidation of fatty acids; carnitine palmitoyl transferase 1a (CPT1a) (Erol et al., 2004; Hsu et al., 2001), which transports fatty acids across the outer mitochondrial membrane; and hydroxymethylglutaryl-CoA synthase 2 (HMGCS2) (Erol et al., 2004; Hsu et al., 2001; Rodriguez et al., 1994), which catalyzes a key step in ketone-body synthesis. Mice lacking PPARα accumulate copious amounts of hepatic triglyceride and become hypoketonemic and hypoglycemic during fasting and starvation (Hashimoto et al., 2000; Kersten et al., 1999; Leone et al., 1999).

Fibroblast growth factor 21 (FGF21) is a member of a subfamily of FGFs, also including FGF15 and FGF23, that function as endocrine hormones (Itoh and Ornitz, 2004; Kharitonenkov et al., 2005). FGF15 and FGF23 have important roles in regulating bile acid and phosphate metabolism, respectively (Houten, 2006; Yu and White, 2005). Recent findings show that FGF21, which is expressed in liver and pancreas, also regulates metabolism. Administration of FGF21 to leptin-deficient rodents decreases

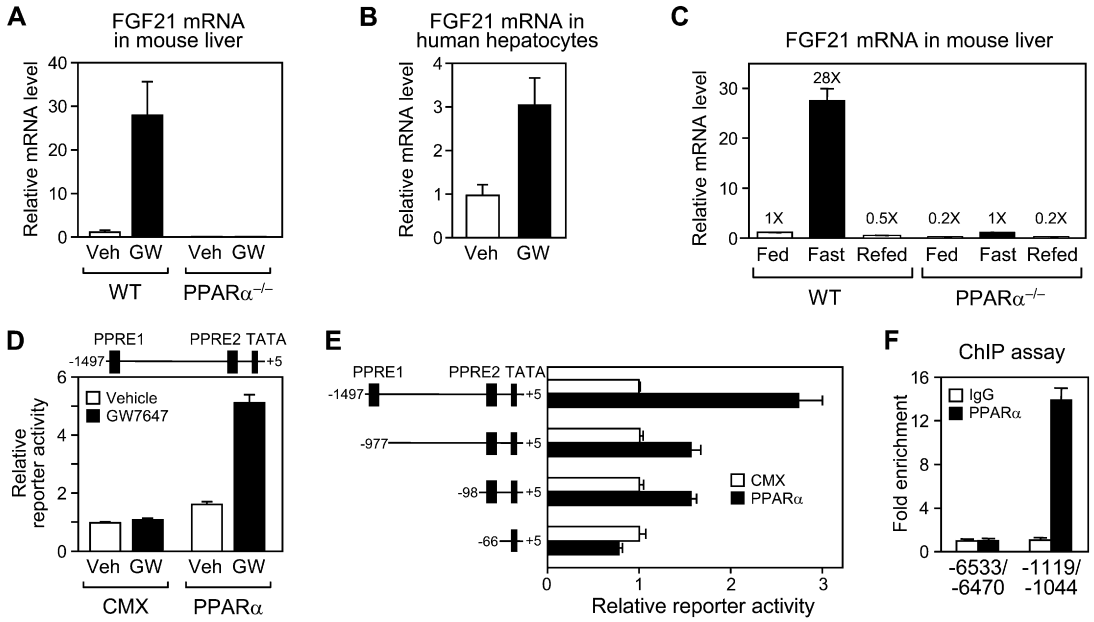

Figure 1. FGF21 mRNA Levels Are Induced during Fasting by PPARα

(A) Wild-type (WT) and *PPARα*$^{-/-}$ mice were administered either GW7647 (GW; 5 mg/kg by oral gavage) or vehicle (Veh) and killed 14 hr later. FGF21 mRNA levels were measured by RT-qPCR. (n = 5 mice per group.) In this and all other figures, error bars represent the mean ± SEM.

(B) Primary cultures of human hepatocytes were treated for 12 hr with GW7647 (GW; 1 μM) or vehicle (Veh). FGF21 mRNA levels were measured by RT-qPCR.

(C) WT and *PPARα*$^{-/-}$ mice were killed in the fed state, after a 12 hr fast, or 12 hr after refeeding. FGF21 mRNA levels were measured by RT-qPCR. (n = 4 mice/group.) The fold induction relative to fed WT mice is shown above each bar.

(D) Cell-based reporter assays were performed in CV-1 cells cotransfected with the FGF21−1497/+5-luciferase reporter in the presence of PPARα expression plasmid or control plasmid (CMX). Cells were treated with either vehicle (white bars) or 100 nM GW7647 (black bars).

(E) Cell-based reporter assays were performed in CV-1 cells cotransfected with the indicated FGF21-luciferase reporter plasmids in the presence of control plasmid (CMX; white bars) or PPARα expression plasmid (black bars). Cells were treated with 100 nM GW7647.

(F) Chromatin immunoprecipitation assays were performed using liver tissue and either PPARα antibodies (black bars) or control IgG (white bars) and primers to the *FGF21* proximal promoter (−1119 to −1044) or a control region (−6533 to −6470).

serum glucose and triglyceride concentrations and enhances insulin sensitivity and glucose clearance (Kharitonenkov et al., 2005). Mice in which FGF21 is overexpressed in liver are resistant to diet-induced weight gain (Kharitonenkov et al., 2005). In diabetic monkeys, FGF21 administration decreases fasting serum glucose, triglyceride, and insulin concentrations and causes small but significant weight loss (Kharitonenkov et al., 2007). It also reduces serum LDL cholesterol levels and raises HDL cholesterol concentrations (Kharitonenkov et al., 2007).

While these studies demonstrate that pharmacological administration of FGF21 has broad metabolic effects, little is known about its physiological function. In this report, we demonstrate that FGF21 is markedly induced by PPARα in liver during fasting to regulate key aspects of the adaptive starvation response.

RESULTS

FGF21 Is Induced during Fasting by PPARα

It was previously shown that the nuclear bile acid receptor FXR regulates *FGF15* in ileum (Inagaki et al., 2005; Li et al., 2005). As part of a systematic analysis to determine whether other nuclear receptors regulate FGFs, we found that PPARα regulates *FGF21* in liver. Real-time quantitative PCR (RT-qPCR) analysis showed that FGF21 mRNA levels were induced ~25-fold in liver in response to GW7647, a PPARα-selective agonist (Brown et al., 2001) (Figure 1A). In *PPARα*$^{-/-}$ mice, basal FGF21 mRNA levels were decreased ~5-fold, and there was no induction by GW7647 (Figure 1A). *FGF21* was also induced by GW7647 in primary cultures of human hepatocytes (Figure 1B). Thus, PPARα regulates *FGF21* in both mouse liver and human hepatocytes. FGF21 mRNA was not increased by GW7647 in pancreas, where it is also expressed (data not shown).

Since PPARα plays a prominent role in the starvation response, we next examined whether *FGF21* is regulated by fasting. FGF21 mRNA levels were increased 28-fold after a 12 hr fast (Figure 1C). Refeeding for 12 hr reduced FGF21 mRNA to prefasting levels. While induction of *FGF21* by fasting was greatly diminished in *PPARα*$^{-/-}$ mice, fasting still caused a 5-fold increase in FGF21 mRNA (Figure 1C). These data demonstrate that *FGF21* is induced during fasting by PPARα but that other pathways also contribute.

PPARα Directly Regulates *FGF21*

To assess whether *FGF21* is regulated directly by PPARα, an *FGF21* promoter fragment extending from −1497 to +5 was used to generate the FGF21−1497/+5-luciferase reporter. In transfection assays performed in CV-1 cells, reporter activity was induced ~5-fold by PPARα in the presence of GW7647 (Figure 1D). Analysis of a series of 5′ deletion mutants showed that truncation of the *FGF21* promoter to −977 resulted in loss of most of the PPARα response, and deletion to −66 eliminated it entirely (Figure 1E). In electrophoretic mobility shift assays, PPARα bound as an RXRα heterodimer to two sequence elements located between −1093 and −1057 and between −98 and −53 (see Figure S1 in the Supplemental Data available with this article online). To determine whether PPARα binds to the *FGF21* promoter in liver, chromatin immunoprecipitation experiments were performed using mouse liver tissue. PPARα binding to the *FGF21* promoter was detected using primers extending from −1119 to −1044, but not with primers that amplify a control region from −6533 to −6470 (Figure 1F). Thus, PPARα directly regulates *FGF21* expression.

FGF21 Induces Ketogenesis

To study the physiological effects of FGF21, transgenic mice were generated in which the mouse *FGF21* coding region was inserted into an apolipoprotein E (*ApoE*) promoter construct that drives transgene expression chronically in the liver (Simonet et al., 1993). As measured by RT-qPCR, FGF21 mRNA was present in liver at ~50-fold higher concentrations in *FGF21* transgenic mice than in fasted wild-type mice (data not shown). The *FGF21* transgenic mice had significant reductions in serum cholesterol, glucose, and insulin (Table S1). These data are similar to those reported recently by another group that independently generated *FGF21* transgenic mice using the *ApoE* promoter (Kharitonenkov et al., 2005).

Since *PPARα*$^{-/-}$ mice have a prominent fasting phenotype that includes impaired ketogenesis and hepatic steatosis (Hashimoto et al., 2000; Kersten et al., 1999; Leone et al., 1999), we measured serum β-hydroxybutyrate and hepatic triglyceride concentrations in wild-type and *FGF21* transgenic mice under fed and fasted conditions. Notably, in the fed state, serum concentrations of β-hydroxybutyrate were increased ~5-fold in *FGF21* transgenic mice compared to wild-type mice (Figure 2A). The increase in ketone-body levels was accompanied by significant decreases in serum and hepatic triglyceride concentrations (Figures 2B and 2C). Under fasted conditions, when endogenous FGF21 is already markedly elevated, only serum triglyceride concentrations were significantly altered between wild-type and *FGF21* transgenic mice (Figures 2A–2C).

The increase in serum β-hydroxybutyrate concentrations in fed *FGF21* transgenic mice suggested that FGF21 induces ketogenesis. To examine this possibility directly, total ketone-body production was measured in isolated perfused livers from fed wild-type and *FGF21* transgenic mice. Ketogenesis was increased ~30% in livers from

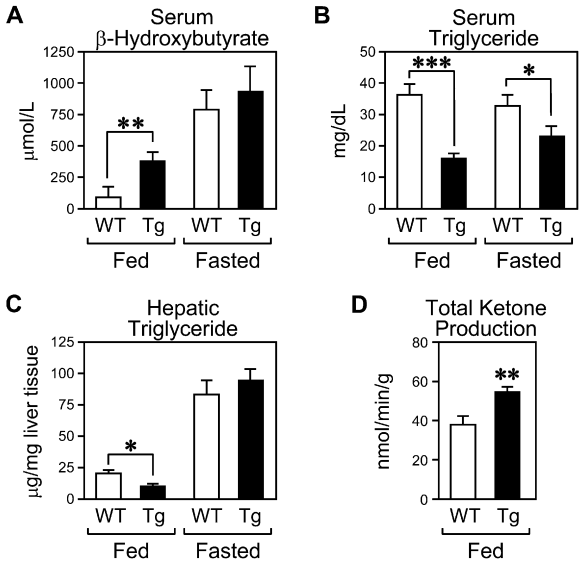

Figure 2. *FGF21* Transgenic Mice Exhibit Increased Ketogenesis

(A–C) Serum β-hydroxybutyrate (A) and triglyceride (B) concentrations and hepatic triglyceride concentrations (C) were measured in wild-type (WT) and *FGF21* transgenic (Tg) mice either in the fed state or after a 24 hr fast. (n = 4 per group.)

(D) Total ketone-body production was measured using perfused livers from WT and Tg mice. (n = 4–5 mice per group.). *p < 0.05; **p < 0.01; ***p < 0.001.

FGF21 transgenic mice (Figure 2D). By comparison, fasting alone induces ketone production by ~60% in isolated rodent livers perfused with 0.5 mM oleate (Scholz et al., 1984). These data suggest that FGF21 contributes substantially to fasting-induced ketogenesis.

We next examined whether shorter-term administration of recombinant FGF21 recapitulates the effects seen in *FGF21* transgenic mice. Wild-type mice and *PPARα*$^{-/-}$ mice, which have low FGF21 mRNA levels in liver (Figure 1A), were injected with recombinant FGF21 or control saline for 3 days, at which point serum β-hydroxybutyrate and triglyceride concentrations were measured in the fed state. After a subsequent 24 hr fast, serum β-hydroxybutyrate and triglyceride levels and hepatic triglyceride concentrations were measured. In the fed state, FGF21 increased serum β-hydroxybutyrate concentrations 2- to 3-fold in both wild-type and *PPARα*$^{-/-}$ mice and caused a corresponding decrease in serum triglyceride concentrations (Figures 3A and 3B). As expected, fasting increased serum β-hydroxybutyrate concentrations in wild-type mice but had no effect in *PPARα*$^{-/-}$ mice (Figure 3A). Whereas FGF21 had no effect on the already high serum β-hydroxybutyrate levels in fasted wild-type mice, it increased β-hydroxybutyrate concentrations ~3-fold in fasted *PPARα*$^{-/-}$ mice, restoring them to ~30% of wild-type levels (Figure 3A). FGF21 administration also caused a significant reduction of triglyceride accumulation in livers of fasted *PPARα*$^{-/-}$ mice (Figure 3C). FGF21 had no effect on the hypoglycemia that occurs in fasted *PPARα*$^{-/-}$ mice

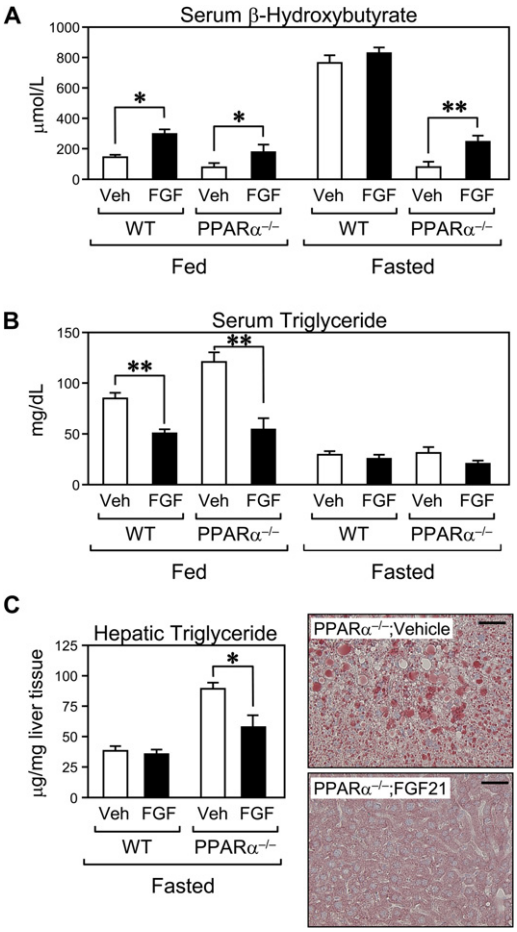

Figure 3. Recombinant FGF21 Injection Induces Ketogenesis

Serum β-hydroxybutyrate (A) and triglyceride (B) concentrations and hepatic triglyceride concentrations (C) were measured in wild-type (WT) and *PPARα*$^{-/-}$ mice administered either FGF21 (FGF; 0.75 mg/kg/day, subcutaneous) or vehicle (Veh) for 3 days. Serum was taken from mice in the fed state or after a 24 hr fast as indicated. (n = 4 mice per group.) *p < 0.05; **p < 0.01. In (C), oil red O-stained liver sections from fasted *PPARα*$^{-/-}$ mice administered either FGF21 or vehicle are shown. Scale bars = 40 μm.

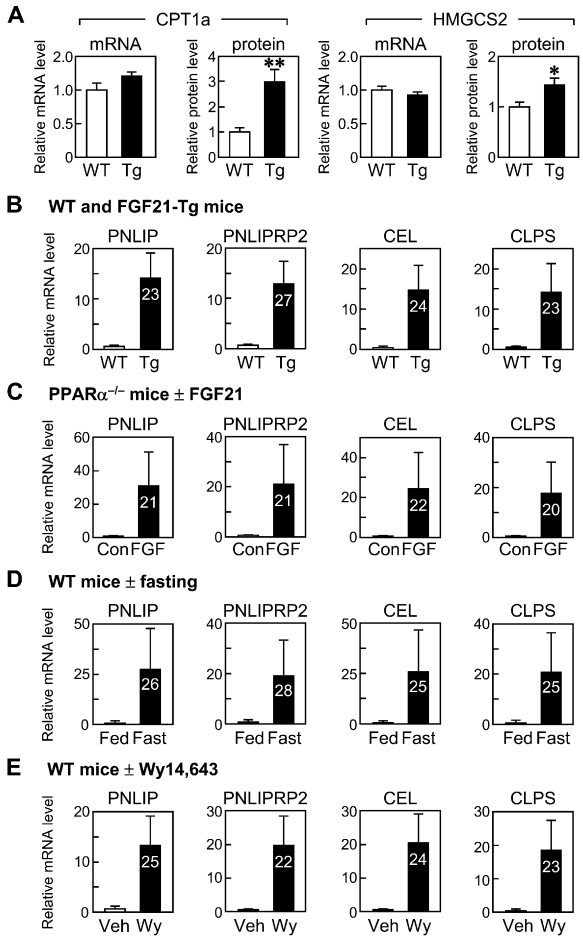

Figure 4. FGF21 Induces Ketogenic Enzymes and Lipases in Liver

(A) CPT1a and HMGCS2 mRNA and protein concentrations in livers from fed wild-type (WT) and *FGF21* transgenic (Tg) mice were measured by RT-qPCR and western blot analysis, respectively. Western data for individual mice are shown in Figure S2. (n = 4 mice per group.) *p < 0.05; **p < 0.01.

(B–E) Pancreatic lipase (PNLIP), pancreatic lipase-related protein 2 (PNLIPRP2), carboxyl ester lipase (CEL), and pancreatic colipase (CLPS) mRNA levels were measured by RT-qPCR in livers from WT and Tg mice (B), *PPARα*$^{-/-}$ mice infected with either control (Con) or FGF21-expressing (FGF) adenoviruses for 5 days (C), WT mice either fed ad libitum or after a 12 hr fast (D), and WT mice administered vehicle (Veh) or the PPARα agonist Wy14,643 (Wy; 0.1% in chow) for 5 days (E). (n = 4–5 mice per group.) Average Ct values are indicated on the bars.

(data not shown). We conclude that FGF21 partially reverses the hypoketonemia and hepatic steatosis that occur during fasting in *PPARα*$^{-/-}$ mice.

FGF21 Induces Lipolysis

Both CPT1a and HMGCS2 mediate crucial steps in ketogenesis (Drynan et al., 1996; Hegardt, 1999), and their genes are regulated directly by PPARα (Erol et al., 2004; Hsu et al., 2001; Rodriguez et al., 1994). Neither CPT1a nor HMGCS2 mRNA levels were significantly changed in *FGF21* transgenic mice compared to wild-type mice (Figure 4A). However, protein concentrations of both CPT1a and HMGCS2 were significantly increased in livers of *FGF21* transgenic mice (Figure 4A and Figure S2), suggesting that FGF21 stimulates ketogenesis in part by increasing CPT1a and HMGCS2 protein levels through a posttranscriptional mechanism.

To understand further how FGF21 induces ketogenesis, microarray experiments were performed using mRNA prepared from livers of wild-type and *FGF21* transgenic mice. No increase in *ACOX1* or other prototypical PPARα target genes was seen (data not shown). Interestingly, however, dramatic increases were observed in the mRNAs encoding a number of pancreatic lipases including pancreatic lipase (PNLIP), pancreatic lipase-related protein 2 (PNLIPRP2), carboxyl ester lipase (CEL), and pancreatic colipase (CLPS). The induction of these lipases was unexpected since they are normally expressed at only very low

levels in liver. RT-qPCR analyses confirmed that hepatic expression of these genes was induced in *FGF21* transgenic mice (Figure 4B), in *PPARα*$^{-/-}$ mice infected with an FGF21-expressing adenovirus (Figure 4C), in wild-type mice fasted for 12 hr (Figure 4D), and in wild-type mice administered the PPARα agonist Wy14,643 for 5 days (Figure 4E). While the Wy14,643 treatment regimen resulted in the expected robust induction of *FGF21* and *ACOX1* (Figure S3), mice fed chow containing Wy14,643 ate ~20% less than mice fed the control diet and weighed ~7% less at the end of the study (data not shown), which complicates interpretation of these results. Nevertheless, these data show that pancreatic lipases are induced by fasting via the PPARα-FGF21 signaling pathway.

The observation that adipocytes from *FGF21* transgenic mice are substantially smaller than those from wild-type mice (Kharitonenkov et al., 2005) (Figure 5A) led us to examine whether FGF21 also regulates lipase expression in WAT. Although PNLIP, PNLIPRP2, CEL, and CLP mRNAs were modestly upregulated in WAT from *FGF21* transgenic mice, no increase was seen in WAT from *PPARα*$^{-/-}$ mice infected with an FGF21-expressing adenovirus (data not shown). However, levels of mRNAs encoding hormone-sensitive lipase (HSL) and adipose triglyceride lipase (ATGL), the two predominant lipases in WAT, were uniformly increased in *FGF21* transgenic mice (Figure 5B), in *PPARα*$^{-/-}$ mice infected with an FGF21-expressing adenovirus (Figure 5C), and in wild-type mice administered Wy14,643 (Figure 5D). Wy14,643 treatment could potentially induce lipase expression in WAT either indirectly by inducing FGF21 in liver or directly by acting on the small amount of PPARα present in WAT. A corresponding increase in HSL and ATGL protein concentrations occurred in WAT from *FGF21* transgenic mice (Figure 5B and Figure S4). Consistent with increased lipase expression and smaller adipocyte size, serum free fatty acid concentrations were significantly increased in *FGF21* transgenic mice and in wild-type mice administered recombinant FGF21 (Figure 5E). Surprisingly, urine concentrations of adrenaline and noradrenaline, which have well-established roles in inducing lipolysis (Collins et al., 2004), were reduced in *FGF21* transgenic mice (Figure S5), indicating that FGF21 does not stimulate lipolysis by causing a systemic increase in catecholamine levels.

To examine directly whether FGF21 induces lipolysis in adipocytes, glycerol release was measured in 3T3-L1 adipocytes treated with either FGF21 or the β-adrenergic receptor agonist isoproterenol. As expected, isoproterenol caused a time-dependent release of glycerol into the media (Figure 5F). Importantly, FGF21 also caused glycerol release, albeit at reduced efficacy compared to isoproterenol (Figure 5F). The 0.5 nM concentration of FGF21 used in these assays was saturating for lipolysis as determined by dose-response analysis (data not shown). Thus, FGF21 stimulates lipolysis in adipocytes. Cotreatment with 0.5 nM FGF21 and 5 nM isoproterenol did not result in any additional stimulation of lipolysis above that seen with isoproterenol alone (Figure S6), suggesting that the two hormones may act through a common pathway. No

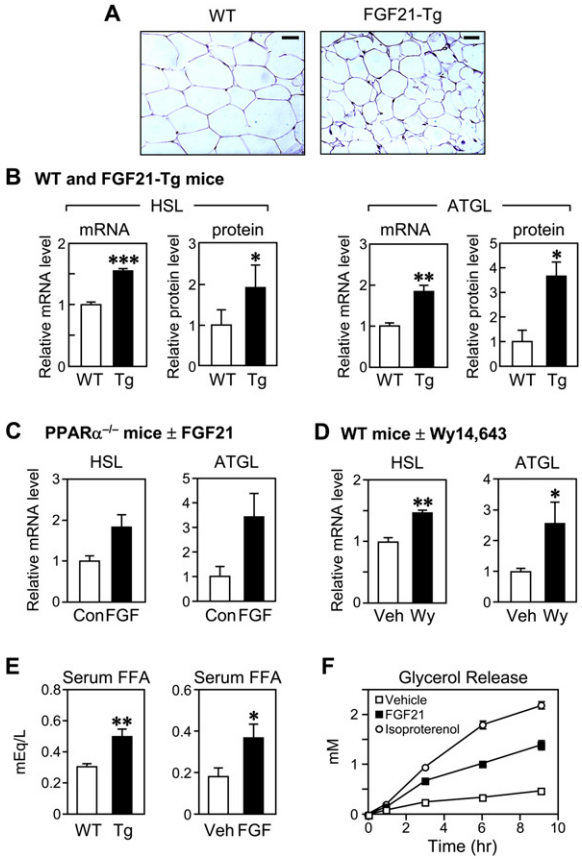

Figure 5. FGF21 Induces Lipolysis in White Adipose Tissue

(A) Hematoxylin and eosin-stained sections of epididymal white adipose tissue (WAT) from wild-type (WT) and *FGF21* transgenic (Tg) mice. Scale bars = 40 μm.

(B) Hormone-sensitive lipase (HSL) and adipose triglyceride lipase (ATGL) mRNA and protein concentrations in epididymal WAT from fed WT and Tg mice were measured by RT-qPCR and western blot analysis, respectively. Western data for individual mice are shown in Figure S4. (n = 4 mice per group.) *p < 0.05; **p < 0.01; ***p < 0.001.

(C and D) HSL and ATGL mRNAs were measured by RT-qPCR in epididymal WAT from *PPARα*$^{-/-}$ mice infected with either control (Con) or FGF21-expressing (FGF) adenovirus for 5 days (C) and WT mice administered vehicle (Veh) or the PPARα agonist Wy14,643 (Wy; 0.1% in chow) for 5 days (D). (n = 4 mice per group.) *p < 0.05; **p < 0.01.

(E) Serum free fatty acid concentrations were measured in fed WT and Tg mice (left panel) or WT mice injected with FGF21 (FGF; 0.75 mg/kg/day, subcutaneous) or vehicle alone (Veh) for 3 days (right panel). (n = 4 mice per group.) *p < 0.05; **p < 0.01.

(F) Glycerol release was measured from 3T3-L1 adipocytes treated with vehicle alone (□), 0.5 nM FGF21 (■), or 5 nM isoproterenol (○) for the indicated times. Assays were performed in triplicate.

increase in HSL or ATGL mRNA levels was seen in response to FGF21 treatment in these in vitro studies (data not shown), indicating that the changes that are seen in the in vivo experiments may be part of an adaptive response to longer-term FGF21 exposure.

FGF21 Enhances Torpor

The pancreatic lipases PNLIPRP2 and CLPS are induced in liver and other tissues during the hibernation-like state

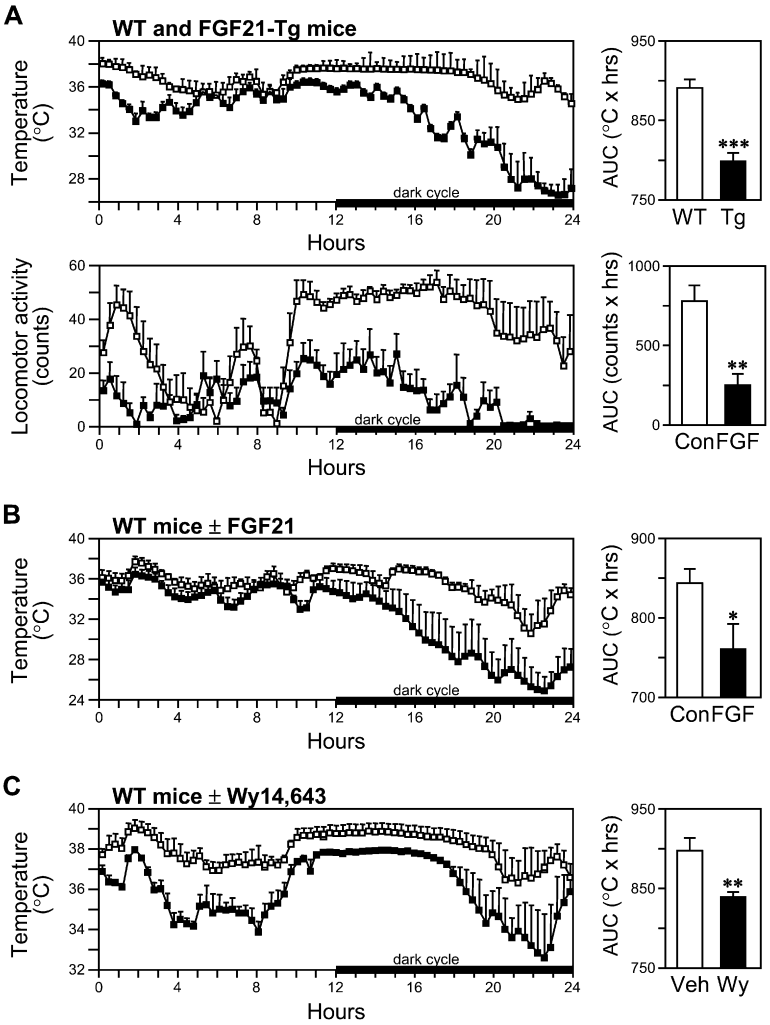

Figure 6. FGF21 Stimulates Torpor

Core body temperature was measured by telemetry in wild-type (WT) mice (open symbols) and *FGF21* transgenic (Tg) mice (closed symbols) fasted for 24 hr ([A], top panel), WT mice infected with a control adenovirus (open symbols) or an FGF21-expressing adenovirus (closed symbols) for 5 days (B), and WT mice treated with vehicle (open symbols) or Wy14,643 (0.1% in chow; closed symbols) for 5 days prior to initiating a 24 hr fast (C). In the bottom panel of (A), locomotor activity was measured during the 24 hr fast. (n = 4 mice per group.) For each experiment, the area under the curve (AUC) for body temperature or locomotor activity during the entire 24 hr period was calculated using GraphPad Prism software. *p < 0.05; **p < 0.01; ***p < 0.001.

of torpor (Zhang et al., 2006). Since FGF21 also induces these lipases, we examined whether it affects torpor by implanting body temperature telemeters in wild-type and *FGF21* transgenic mice. The basal core body temperature of *FGF21* transgenic mice was consistently 1°C–2°C lower than that of wild-type mice (Figure 6A, top panel). Moreover, during a 24 hr fast, *FGF21* transgenic mice entered torpor, whereas wild-type mice did not (Figure 6A, top panel). A similar induction of torpor was observed in wild-type mice infected with an FGF21-expressing adenovirus compared to a control adenovirus (Figure 6B). To examine whether core body temperature is also affected under conditions in which endogenous FGF21 is increased, telemetry experiments were performed in wild-type mice treated with either the PPARα agonist Wy14,643 or vehicle alone. Administration of Wy14,643 resulted in reductions in both basal and fasting-induced body temperature (Figure 6C). However, as noted above, mice fed chow containing Wy14,643 were hypophagic and weighed less at the end of the study than mice fed the control diet, complicating interpretation of these results. Taken together, the telemetry data demonstrate that FGF21 stimulates fasting-induced torpor.

To examine whether the FGF21-induced changes in body temperature are associated with decreased physical movement, locomotor activity was measured in wild-type and *FGF21* transgenic mice during a 24 hr fast. Interestingly, locomotor activity was dramatically reduced in *FGF21* transgenic mice (Figure 6A, bottom panel). These data reveal that FGF21 alters behavior to conserve energy and suggest that it reduces body temperature in part by decreasing physical activity.

DISCUSSION

It is well established that PPARα plays a central role in the starvation response by directly stimulating the transcription of genes involved in fatty acid oxidation and ketone-body production (Kersten et al., 2000; Lefebvre et al., 2006). In this report, evidence is presented that PPARα plays an even broader role during starvation by inducing the hormone FGF21 in liver. Gain-of-function experiments reveal that FGF21 regulates diverse processes associated with fasting and energy conservation including lipolysis, ketogenesis, physical activity, and torpor. In the accompanying paper by Badman et al. (2007) in this issue of

Cell Metabolism, complementary loss-of-function experiments demonstrate that FGF21 is required for maximal hepatic lipid oxidation and ketogenesis induced by a ketogenic diet. These two alternative approaches show that the PPARα-FGF21 signaling cascade regulates ketogenesis caused by either fasting or dietary manipulation and further suggest that this pathway is an important component of the adaptive response to long-term nutrient deprivation.

FGF21 and Ketogenesis

While ketone bodies are a crucial energy source during fasting and starvation, their overproduction causes ketoacidosis, which can lead to coma and death. Thus, ketogenesis must be tightly coupled to energy demands. Much of the regulation of ketogenesis during starvation is mediated directly by PPARα, which induces *HMGCS2*, *CPT1a*, and numerous other genes required for fatty acid oxidation and metabolism by binding directly to DNA response elements in their promoters (Erol et al., 2004; Hashimoto et al., 2000; Hsu et al., 2001; Kersten et al., 1999; Leone et al., 1999; Rodriguez et al., 1994). We now present evidence that PPARα also promotes ketone-body production by inducing FGF21. Unlike PPARα, FGF21 did not stimulate ketogenesis by increasing mRNAs encoding CPT1a, HMGCS2, or other proteins involved in fatty acid oxidation. Thus, FGF21 induces ketone-body production through a mechanism distinct from that previously described for PPARα. Notably, protein levels of HMGCS2 and CPT1a were significantly increased in livers of *FGF21* transgenic mice, suggesting a molecular basis for at least part of the effect of FGF21 on ketone-body production.

Previous studies showed that infusion of exogenous fatty acids or induction of lipolysis without changing the activity of the ketogenic enzymes is sufficient to induce ketogenesis (Avogaro et al., 1992; Bates et al., 1976; Beylot et al., 1987). Several lines of evidence indicate that FGF21 also induces ketogenesis by stimulating lipolysis, thereby increasing the supply of free fatty acids to the liver. First, *FGF21* transgenic mice have markedly smaller white adipocytes than their wild-type counterparts, suggesting that the adipocytes are depleted of lipid (Kharitonenkov et al., 2005). Second, both *FGF21* transgenic mice and wild-type mice administered recombinant FGF21 had significant increases in serum free fatty acid concentrations, indicative of increased lipolysis. Third, FGF21 enhanced lipolysis in 3T3-L1 adipocytes, suggesting that FGF21 acts directly on WAT to stimulate lipolysis.

FGF21 was previously shown to stimulate glucose uptake in 3T3-L1 adipocytes (Kharitonenkov et al., 2005). The finding that FGF21 stimulates both glucose uptake and lipolysis in adipocytes—and causes corresponding increases in insulin sensitivity and circulating free fatty acid levels in vivo—is surprising since these processes are regulated in opposite directions by both insulin and catecholamines. FGF21 was shown previously to increase glucose transporter 1 expression in adipocytes, which may account for its effects on glucose uptake (Kharitonenkov et al., 2005). However, the mechanisms underlying its lipolytic actions remain unclear. Adrenaline and noradrenaline concentrations were reduced in urine of *FGF21* transgenic mice, indicating that FGF21 does not cause systemic increases in catecholamines. While mRNA and protein levels of HSL and ATGL were increased in WAT of *FGF21* transgenic mice, they were not induced by FGF21 in 3T3-L1 adipocytes in short-term experiments in which lipolysis was increased. Additional studies will be required to determine how FGF21 stimulates lipolysis and the relationship between its effects on glucose and fatty acid metabolism.

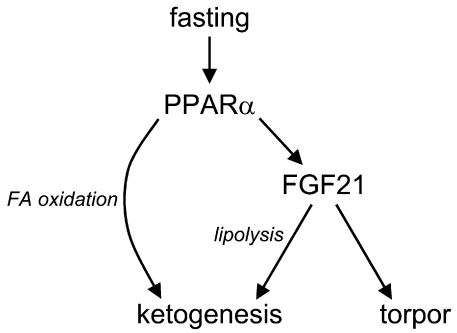

Figure 7. Model for the Coordinate Actions of PPARα and FGF21 during Fasting

In liver, PPARα directly induces transcription of enzymes and transporters required for fatty acid (FA) oxidation and ketogenesis. PPARα also induces FGF21, which through endocrine and autocrine/paracrine mechanisms promotes lipolysis in white adipose tissue and liver, stimulates ketogenesis in liver, and enhances torpor.

A role for FGF21 in increasing hepatic concentrations of free fatty acids is also supported by its effects in liver. FGF21 caused striking increases in hepatic levels of mRNAs encoding the pancreatic lipases PNLIP, PNLIPRP2, and CEL. During fasting, a substantial fraction of free fatty acids taken up by the liver are re-esterified to triglyceride (Baar et al., 2005). Thus, induction of lipases by FGF21 may provide a mechanism for the efficient hydrolysis of hepatic triglyceride stores, especially during long-term nutritional deficiency (see below). Consistent with this hypothesis, FGF21 administration caused a significant reduction in the hepatic hypertriglyceridemia that occurs in fasted *PPARα*$^{-/-}$ mice.

Based on all of the data, we propose the following model for how PPARα induces ketogenesis during fasting (see Figure 7). In liver, PPARα directly stimulates the transcription of *CPT1a*, *HMGCS2*, and other genes involved in the uptake and catabolism of fatty acids by binding to DNA response elements in their promoters. PPARα also induces hepatic expression of FGF21, which acts in an autocrine/paracrine fashion to increase CPT1a, HMGCS2, and pancreatic lipase levels in liver and in an endocrine manner to stimulate lipolysis in WAT. The net result of this bipartite mechanism is the stimulation of ketogenesis by increasing both the supply of free fatty acids to the liver and the concentrations of proteins required for ketone-body production.

FGF21 and Torpor

Our finding that FGF21 induces pancreatic lipases in liver was interesting in light of a recent report that PNLIPRP2 and CLPS are also induced in mouse liver during torpor, the murine equivalent of hibernation (Zhang et al., 2006). These data, together with the finding that *PNLIP* is induced in extrapancreatic tissues by hibernation in ground squirrels (Andrews et al., 1998; Bauer et al., 2001), suggested that FGF21 might regulate torpor. Indeed, *FGF21* transgenic mice entered torpor during fasting, whereas wild-type mice did not. Infection of mice with an FGF21-expressing adenovirus also stimulated torpor. Notably, ketone-body concentrations are markedly elevated during torpor and hibernation (Krilowicz, 1985; Rauch and Behrisch, 1981). Thus, FGF21 regulates key aspects of the global torpor response including lipase expression, ketogenesis, and body temperature.

Why are pancreatic lipases induced in other tissues during torpor and hibernation? One possible reason is the unique biochemical properties of these lipases, which evolved to function in the harsh conditions encountered in the gut. For example, PNLIP is 10-fold more efficient than HSL at hydrolyzing triglycerides and retains full activity at temperatures as low as 0°C (Andrews et al., 1998; Fredrikson et al., 1981). Moreover, the activities of PNLIP and other pancreatic lipases are unaffected by catecholamines, which are ineffective at stimulating lipolysis at low temperatures (Dark et al., 2003; Moreau-Hamsany et al., 1988). Thus, the extrapancreatic induction of pancreatic lipases by FGF21 may ensure the continuous delivery of free fatty acids to tissues even under adverse environmental conditions in which the conventional catecholamine-regulated lipase pathways are compromised.

Broader Implications of the PPARα-FGF21 Pathway

The studies presented in this paper focus on the roles of the PPARα-FGF21 pathway in regulating fatty acid metabolism, ketogenesis, and torpor. The similar effects of PPARα agonists and FGF21 on these parameters, together with the finding that FGF21 partially reverses the hypoketonemia and hypertriglyceridemia in *PPARα*$^{-/-}$ mice, suggest that FGF21 contributes to the pleiotropic actions of PPARα. Additional similarities in the pharmacological profiles of PPARα agonists and FGF21 further suggest that the implications of this signaling cascade are likely to be broader. For example, both fibrates and FGF21 lower LDL cholesterol, raise HDL cholesterol, and improve insulin sensitivity in dyslipidemic rhesus monkeys (Kharitonenkov et al., 2007; Winegar et al., 2001). Furthermore, both PPARα agonists and FGF21 prevent diet-induced obesity and enhance insulin sensitivity in rodents (Chou et al., 2002; Guerre-Millo et al., 2000; Kharitonenkov et al., 2005; Tsuchida et al., 2005). This striking overlap in activities suggests that FGF21 contributes to many of the actions of PPARα agonists. The finding that *FGF21* is induced by PPARα in human hepatocytes raises the intriguing possibility that FGF21 also contributes to the therapeutic actions of the fibrate drugs.

In closing, the identification of the PPARα-FGF21 signaling cascade reveals an unexpected endocrine pathway originating in the liver that regulates diverse components of the adaptive starvation response, including ketogenesis and torpor. Moreover, this finding extends the relationship between nuclear receptors and the FGF15/21/23 subfamily of endocrine hormones. It was previously shown that the bile acid receptor FXR induces FGF15 to regulate bile acid homeostasis (Inagaki et al., 2005; Li et al., 2005) and that the vitamin D receptor induces FGF23 to regulate phosphate and vitamin D homeostasis (Kolek et al., 2005). The finding that FGF21 is regulated by PPARα demonstrates that each member of this unusual FGF subfamily is regulated by a corresponding nuclear receptor. The induction of endocrine FGFs provides a mechanism for nuclear receptors to extend their biological actions to tissues in which they are not expressed and thereby coordinate complex physiological responses.

EXPERIMENTAL PROCEDURES

Animal Experiments

All experiments were performed with male mice. *PPARα*$^{-/-}$ mice on a pure 129S4/Sv background were purchased from The Jackson Laboratory. Mice were fed standard chow containing 4% fat ad libitum. All animal experiments were approved by the Institutional Animal Care and Research Advisory Committee of the University of Texas Southwestern Medical Center.

For the fasting and refeeding experiment presented in Figure 1C, mice were divided into three groups: nonfasted, fasted, and refed. The nonfasted group was fed ad libitum, the fasted group was fasted for 12 hr, and the refed group was fasted for 12 hr and then refed regular chow diet for 12 hr. The starting times for the feeding regimens were staggered so that all mice were killed at the same time at the end of the dark cycle. Liver mRNA prepared from the 12 hr fed and fasted groups was also used for the RT-qPCR experiments shown in Figure 4D. For all other fasting experiments, mice were fasted for 24 hr and killed at the end of dark cycle. For experiments with Wy14,643 (Chemsyn Science Laboratories), mice were fed chow with 0.1% Wy14,643 admixed. For core body temperature and locomotor activity measurements, TAF2 telemetric temperature transmitters (Data Sciences International) were implanted in the peritoneal cavity under general anesthesia. Mice were allowed to recover for >7 days. Data from mice individually housed at 22°C were collected and analyzed using ART2.1 software (Data Sciences International).

To generate the *FGF21* transgenic mice, a cDNA containing the mouse *FGF21* coding region was inserted into the MluI and XhoI sites of pLiv7 (Miyake et al., 2001; Simonet et al., 1993). The 6.7 kb SalI-SpeI fragment of pLiv7-FGF21 was injected into fertilized eggs as previously described (Shimano et al., 1996). Transgenic mice were generated and maintained on a C57BL/6J background. Two independent *FGF21* transgenic mouse lines were established that had hepatic FGF21 mRNA concentrations ~50-fold (line 1) and ~150-fold higher (line 2) than those in fasted wild-type mice. The two lines had virtually identical changes in fasting serum β-hydroxybutyrate, triglyceride, total cholesterol, glucose, and insulin concentrations (data not shown). All additional experiments were performed with line 1.

Recombinant FGF21

Recombinant mouse FGF21 (residues 33–209) was expressed in *E. coli*, refolded in vitro, and purified to homogeneity by sequential affinity, ion exchange, and size exclusion chromatography as previously described (Plotnikov et al., 2000).

Adenovirus Infections

The *FGF21* coding region was cloned into the pACCMVpLpA(−)loxP vector at unique BamHI and HindIII sites. Virus was propagated and purified as described (Aoki et al., 1999; Gerard and Meidell, 1995). Mice were infected with adenovirus by jugular vein injection using a 3/10 cc syringe (Becton, Dickinson and Company). Each mouse received 7.5×10^9 particles/g body weight in 0.1 ml of saline. Four days after injection, mice were kept under fed or fasted conditions for 24 hr.

Metabolite Measurements

Total lipids were extracted from ~50 mg of liver as previously described (Folch et al., 1957). Triglyceride content of liver and plasma triglyceride concentrations were measured using an L-type TG H triglyceride kit (Wako Chemicals Inc.). Plasma free fatty acids were measured using a NEFA C kit (Wako Chemicals Inc.). Plasma β-hydroxybutyrate concentrations were measured using a D-3-hydroxybutyric acid kit (R-Biopharm AG).

Perfused Liver Experiments

Livers from fed *FGF21* transgenic mice or wild-type littermates were isolated and perfused for 60 min in a nonrecirculating fashion at 8 ml/min with a Krebs-Henseleit-based perfusion medium containing 1.5 mM lactate, 0.15 mM pyruvate, 0.25 mM glycerol, and 0.4 mM free fatty acid (algal mix bound to 3% albumin) as described (Burgess et al., 2004). Ketone production was determined by standard biochemical assays of the effluent perfusate.

Human Hepatocytes

Human primary hepatocytes were obtained from the Liver Tissue Procurement and Distribution System as attached cells in six-well plates in human hepatocyte maintenance medium (Cambrex Bio Science Walkersville Inc.) supplemented with 100 nM dexamethasone, 100 nM insulin, 100 U/ml penicillin G, and 100 μg/ml streptomycin. Twelve hours after changing the culture medium to serum-free Williams' E medium, cells were treated with 1 μM GW7647 or vehicle (0.1% DMSO).

Plasmids and Transient Transfection Assays

The *FGF21* promoter constructs −1497/+5, −977/+5, and −98/+5 were generated by PCR using 129Sv mouse genomic DNA and the following oligonucleotides: −1497 forward, 5′-GACGGCAAGCTTGGCCTGAAGCCTCACCTTGAC-3′; −977 forward, 5′-CCCAAGCTTCCAAAGCACCTTGTAGCTTAA-3′; −98 forward, 5′-GACGGCAAGCTTGGTTCCTGCCAAGTGTGTC-3′; +5 reverse, 5′-GACGGCCTCGAGTGTCTGGTGAACGCAGAAATACCC-3′. The PCR-amplified fragments were cloned into a luciferase reporter construct using HindIII and XhoI sites. To generate the −66/+5 fragment, the following oligonucleotides were synthesized and annealed: forward, 5′-AGCTTCAGGAGTGGGGAGGGCACGTGGGCGGGCCTGTCTGGGTATAAATTCTGGGTATTTCTGCGTTCACCAGACAC-3′; reverse, 5′-TCGAGTGTCTGGTGAACGCAGAAATACCCAGAATTTATACCCAGACAGGCCCGCCCACGTGCCCTCCCCACTCCTGA-3′. The annealed oligonucleotides were cloned into a luciferase reporter using HindIII and XhoI sites. All constructs were verified by DNA sequencing.

For transient transfection assays, CV-1 cells were maintained in DMEM containing 10% fetal bovine serum supplemented with L-glutamine and antibiotics. Cells were plated in 96-well plates at a density of 10,000 cells per well. After 24 hr, cells were transfected using Lipofectamine 2000 (Invitrogen). Each well was transfected with 20 ng of *FGF21* reporter gene, 5 ng of CMX or CMX-mouse PPARα, and 20 ng of CMV-β-galactosidase. pGEM was added to bring the total DNA to 110 ng/well. After overnight transfection, cells were treated with GW7647 or vehicle alone (0.1% DMSO) in delipidated medium for 24 hr before performing luciferase and β-galactosidase assays. Luciferase activity was normalized to β-galactosidase activity.

Chromatin Immunoprecipitation

Frozen adult mouse liver was crushed into powder. DNA-protein crosslinking was performed by incubating powdered liver tissue (50 mg) with 1% formaldehyde in PBS containing 1 mM DTT and 1 mM PMSF for 10–15 min at room temperature with gentle shaking. Crosslinking reactions were stopped by adding glycine to 0.125 M. Liver nuclei were isolated with a Dounce homogenizer in hypotonic solution followed by centrifugation at 4000 × g for 1 min. Chromatin immunoprecipitation assays were performed with liver nuclei using a ChIP assay kit (Upstate Biotechnology) and anti-PPARα antibody (5 μg, Affinity BioReagents) or control rabbit IgG (Santa Cruz Biotechnology). Precipitated DNA was purified using a spin column (QIAGEN) and eluted in 100 μl water. DNA (1.25 μl) was subjected to RT-qPCR analysis as described (Bookout and Mangelsdorf, 2003) using the following oligonucleotides: *FGF21* −6533/−6470 forward, 5′-TCAGCATGCCTCCAAAGC-3′, reverse, 5′-TCAGCCTTGAGGAAGAGTAGACA-3′; *FGF21* −1119/−1044 forward, 5′-AGGGCCCGAATGCTAAGC-3′; reverse, 5′-AGCCAAGCAGGTGGAAGTCT-3′.

In Vitro Lipolysis Assay

3T3-L1 mouse fibroblasts were differentiated into adipocytes using a standard differentiation protocol (Student et al., 1980). Briefly, cells were grown to confluency and incubated for 2 days in an induction cocktail consisting of DMEM with 10% FBS, 10 μg/ml insulin, 0.5 mM IBMX, and 0.25 μM dexamethasone. Cells were maintained in differentiation media consisting of DMEM with 10% FBS and 10 μg/ml insulin for 4 days, followed by a 2 day incubation in DMEM with 10% FBS alone. Glycerol release was measured using an adipolysis assay kit (Chemicon).

RT-qPCR Analysis

Primers were designed using Primer Express software (Applied Biosystems) based on GenBank sequence data. All primer sequences were BLASTed against the NCBI mouse genomic sequence database to ensure unique specificity. Primer sequences are listed in Table S2. RT-qPCR reactions (10 μl) contained 25 ng of cDNA, 150 nM of each primer, and 5 μl of SYBR Green PCR Master Mix (Applied Biosystems). All reactions were performed in triplicate on an Applied Biosystems Prism 7700HT sequence detection system, and relative mRNA levels were calculated by the comparative threshold cycle method by using cyclophilin or apolipoprotein B as the internal control (Bookout and Mangelsdorf, 2003).

Immunoblot Analysis

For CPT1a and HMGCS2 immunoblotting, 100 mg of liver was homogenized in 1 ml buffer A (10 mM Tris-HCl [pH 7.4], 5 mM EDTA, 150 mM NaCl, 30 mM sodium phosphate, 10% glycerol, 0.5% NP40 containing Complete protease inhibitor cocktail [Roche Diagnostics]) using a Polytron homogenizer. After centrifugation at 16,000 × g for 5 min at 4°C, the supernatant was collected. Immunoblotting was performed using antibodies against CPT1a (Esser et al., 1993), HMGCS2 (Santa Cruz Biotechnology), and β-actin (Sigma-Aldrich). For HSL and ATGL immunoblotting, epididymal WAT was homogenized in buffer A. Samples were centrifuged at 16,000 × g for 25 min at 4°C, and the supernatant was collected. Immunoblotting was performed using antibodies against HSL (Santa Cruz Biotechnology), ATGL (Cell Signaling Technology), and β-actin (Sigma-Aldrich).

Statistical Analyses

Statistical analyses were performed using Minitab Release 14 software (Minitab Inc.). Comparisons of two groups were performed using Student's t test. $p < 0.05$ was considered significant.

Supplemental Data

Supplemental Data include two tables and six figures and can be found with this article online at http://www.cellmetabolism.org/cgi/content/full/5/6/415/DC1/.

ACKNOWLEDGMENTS

We thank L. Peng for technical assistance; N. Anderson and J. Horton for microarray analysis; J. Richardson, J. Shelton, and the UTSW Molecular Pathology Core Laboratory for histology and analysis; J. Repa for reagents and assistance during the early stages of this work; the UTSW Transgenic Core Facility; T. Willson (GlaxoSmithKline) for GW7647; and S. Strom (University of Pittsburgh) and the Liver Tissue Procurement and Distribution System (NIH grant DK92310) for human hepatocytes. We also thank E. Maratos-Flier and J. Flier for sharing unpublished data. This work was funded by NIH grants DK067158 (S.A.K.), P20RR20691 (S.A.K. and D.J.M.), U19DK62434 (D.J.M.), DK53301 (J.K.E.), U24DK076169 (S.C.B.), and DE13686 (M.M.); the Robert A. Welch Foundation (S.A.K. and D.J.M.); the Betty Van Andel Foundation (Y.L.); the Smith Family Foundation Pinnacle Program Project Award from the American Diabetes Association (J.K.E.); and the Howard Hughes Medical Institute (X.D. and D.J.M.). D.J.M. is an investigator of the Howard Hughes Medical Institute.

Received: January 17, 2007
Revised: March 28, 2007
Accepted: May 3, 2007
Published: June 5, 2007

REFERENCES

Andrews, M.T., Squire, T.L., Bowen, C.M., and Rollins, M.B. (1998). Low-temperature carbon utilization is regulated by novel gene activity in the heart of a hibernating mammal. Proc. Natl. Acad. Sci. USA *95*, 8392–8397.

Aoki, K., Barker, C., Danthinne, X., Imperiale, M.J., and Nabel, G.J. (1999). Efficient generation of recombinant adenoviral vectors by Cre-lox recombination in vitro. Mol. Med. *5*, 224–231.

Avogaro, A., Cryer, P.E., and Bier, D.M. (1992). Epinephrine's ketogenic effect in humans is mediated principally by lipolysis. Am. J. Physiol. *263*, E250–E260.

Baar, R.A., Dingfelder, C.S., Smith, L.A., Bernlohr, D.A., Wu, C., Lange, A.J., and Parks, E.J. (2005). Investigation of in vivo fatty acid metabolism in AFABP/aP2(−/−) mice. Am. J. Physiol. Endocrinol. Metab. *288*, E187–E193.

Badman, M.K., Pissios, P., Kennedy, A.R., Koukos, G., Flier, J.S., and Maratos-Flier, E. (2007). Hepatic fibroblast growth factor 21 is regulated by PPARα and is a key mediator of hepatic lipid metabolism in ketotic states. Cell Metab. *5*, this issue, 426–437.

Bates, M.W., Linn, L.C., and Huen, A.H. (1976). Effects of oleic acid infusion on plasma free fatty acids and blood ketone bodies in the fasting rat. Metabolism *25*, 361–373.

Bauer, V.W., Squire, T.L., Lowe, M.E., and Andrews, M.T. (2001). Expression of a chimeric retroviral-lipase mRNA confers enhanced lipolysis in a hibernating mammal. Am. J. Physiol. Regul. Integr. Comp. Physiol. *281*, R1186–R1192.

Beylot, M., Beaufrere, B., Riou, J.P., Khalfallah, Y., Moneger, A., Odeon, M., Cohen, R., and Mornex, R. (1987). Effect of epinephrine on the relationship between nonesterified fatty acid availability and ketone body production in postabsorptive man: evidence for a hepatic antiketogenic effect of epinephrine. J. Clin. Endocrinol. Metab. *65*, 914–921.

Bookout, A.L., and Mangelsdorf, D.J. (2003). Quantitative real-time PCR protocol for analysis of nuclear receptor signaling pathways. Nucl. Recept. Signal. *1*, e012.

Brown, P.J., Stuart, L.W., Hurley, K.P., Lewis, M.C., Winegar, D.A., Wilson, J.G., Wilkison, W.O., Ittoop, O.R., and Willson, T.M. (2001). Identification of a subtype selective human PPARalpha agonist through parallel-array synthesis. Bioorg. Med. Chem. Lett. *11*, 1225–1227.

Burgess, S.C., Hausler, N., Merritt, M., Jeffrey, F.M., Storey, C., Milde, A., Koshy, S., Lindner, J., Magnuson, M.A., Malloy, C.R., and Sherry, A.D. (2004). Impaired tricarboxylic acid cycle activity in mouse livers lacking cytosolic phosphoenolpyruvate carboxykinase. J. Biol. Chem. *279*, 48941–48949.

Cahill, G.F. (2006). Fuel metabolism in starvation. Annu. Rev. Nutr. *26*, 1–22.

Chou, C.J., Haluzik, M., Gregory, C., Dietz, K.R., Vinson, C., Gavrilova, O., and Reitman, M.L. (2002). WY14,643, a peroxisome proliferator-activated receptor alpha (PPARalpha) agonist, improves hepatic and muscle steatosis and reverses insulin resistance in lipoatrophic A-ZIP/F-1 mice. J. Biol. Chem. *277*, 24484–24489.

Collins, S., Cao, W., and Robidoux, J. (2004). Learning new tricks from old dogs: beta-adrenergic receptors teach new lessons on firing up adipose tissue metabolism. Mol. Endocrinol. *18*, 2123–2131.

Dark, J., Miller, D.R., Lewis, D.A., Fried, S.K., and Bunkin, D. (2003). Noradrenaline-induced lipolysis in adipose tissue is suppressed at hibernation temperatures in ground squirrels. J. Neuroendocrinol. *15*, 451–458.

Drynan, L., Quant, P.A., and Zammit, V.A. (1996). Flux control exerted by mitochondrial outer membrane carnitine palmitoyltransferase over beta-oxidation, ketogenesis and tricarboxylic acid cycle activity in hepatocytes isolated from rats in different metabolic states. Biochem. J. *317*, 791–795.

Erol, E., Kumar, L.S., Cline, G.W., Shulman, G.I., Kelly, D.P., and Binas, B. (2004). Liver fatty acid binding protein is required for high rates of hepatic fatty acid oxidation but not for the action of PPARalpha in fasting mice. FASEB J. *18*, 347–349.

Esser, V., Kuwajima, M., Britton, C.H., Krishnan, K., Foster, D.W., and McGarry, J.D. (1993). Inhibitors of mitochondrial carnitine palmitoyltransferase I limit the action of proteases on the enzyme. Isolation and partial amino acid analysis of a truncated form of the rat liver isozyme. J. Biol. Chem. *268*, 5810–5816.

Folch, J., Lees, M., and Sloane Stanley, G.H. (1957). A simple method for the isolation and purification of total lipides from animal tissues. J. Biol. Chem. *226*, 497–509.

Fredrikson, G., Stralfors, P., Nilsson, N.O., and Belfrage, P. (1981). Hormone-sensitive lipase of rat adipose tissue. Purification and some properties. J. Biol. Chem. *256*, 6311–6320.

Fukao, T., Lopaschuk, G.D., and Mitchell, G.A. (2004). Pathways and control of ketone body metabolism: on the fringe of lipid biochemistry. Prostaglandins Leukot. Essent. Fatty Acids *70*, 243–251.

Geiser, F. (2004). Metabolic rate and body temperature reduction during hibernation and daily torpor. Annu. Rev. Physiol. *66*, 239–274.

Gerard, R.D., and Meidell, R.S. (1995). Adenovirus vectors. In DNA Cloning 4: A Practical Approach: Mammalian Systems, D.M. Glover and B.D. Hames, eds. (Oxford: Oxford University Press), pp. 285–307.

Guerre-Millo, M., Gervois, P., Raspe, E., Madsen, L., Poulain, P., Derudas, B., Herbert, J.M., Winegar, D.A., Willson, T.M., Fruchart, J.C., et al. (2000). Peroxisome proliferator-activated receptor alpha activators improve insulin sensitivity and reduce adiposity. J. Biol. Chem. *275*, 16638–16642.

Hashimoto, T., Cook, W.S., Qi, C., Yeldandi, A.V., Reddy, J.K., and Rao, M.S. (2000). Defect in peroxisome proliferator-activated receptor alpha-inducible fatty acid oxidation determines the severity of hepatic steatosis in response to fasting. J. Biol. Chem. *275*, 28918–28928.

Hegardt, F.G. (1999). Mitochondrial 3-hydroxy-3-methylglutaryl-CoA synthase: a control enzyme in ketogenesis. Biochem. J. *338*, 569–582.

Houten, S.M. (2006). Homing in on bile acid physiology. Cell Metab. *4*, 423–424.

Hsu, M.H., Savas, U., Griffin, K.J., and Johnson, E.F. (2001). Identification of peroxisome proliferator-responsive human genes by elevated expression of the peroxisome proliferator-activated receptor alpha in HepG2 cells. J. Biol. Chem. *276*, 27950–27958.

Inagaki, T., Choi, M., Moschetta, A., Peng, L., Cummins, C.L., McDonald, J.G., Luo, G., Jones, S.A., Goodwin, B., Richardson, J.A., et al.

(2005). Fibroblast growth factor 15 functions as an enterohepatic signal to regulate bile acid homeostasis. Cell Metab. *2*, 217–225.

Itoh, N., and Ornitz, D.M. (2004). Evolution of the Fgf and Fgfr gene families. Trends Genet. *20*, 563–569.

Kersten, S., Seydoux, J., Peters, J.M., Gonzalez, F.J., Desvergne, B., and Wahli, W. (1999). Peroxisome proliferator-activated receptor alpha mediates the adaptive response to fasting. J. Clin. Invest. *103*, 1489–1498.

Kersten, S., Desvergne, B., and Wahli, W. (2000). Roles of PPARs in health and disease. Nature *405*, 421–424.

Kharitonenkov, A., Shiyanova, T.L., Koester, A., Ford, A.M., Micanovic, R., Galbreath, E.J., Sandusky, G.E., Hammond, L.J., Moyers, J.S., Owens, R.A., et al. (2005). FGF-21 as a novel metabolic regulator. J. Clin. Invest. *115*, 1627–1635.

Kharitonenkov, A., Wroblewski, V.J., Koester, A., Chen, Y.F., Clutinger, C.K., Tigno, X.T., Hansen, B.C., Shanafelt, A.B., and Etgen, G.J. (2007). The metabolic state of diabetic monkeys is regulated by fibroblast growth factor-21. Endocrinology *148*, 774–781. Published online October 26, 2006. 10.1210/en.2006-1168.

Kolek, O.I., Hines, E.R., Jones, M.D., LeSueur, L.K., Lipko, M.A., Kiela, P.R., Collins, J.F., Haussler, M.R., and Ghishan, F.K. (2005). 1alpha,25-Dihydroxyvitamin D3 upregulates FGF23 gene expression in bone: the final link in a renal-gastrointestinal-skeletal axis that controls phosphate transport. Am. J. Physiol. Gastrointest. Liver Physiol. *289*, G1036–G1042.

Krilowicz, B.L. (1985). Ketone body metabolism in a ground squirrel during hibernation and fasting. Am. J. Physiol. *249*, R462–R470.

Lefebvre, P., Chinetti, G., Fruchart, J.C., and Staels, B. (2006). Sorting out the roles of PPAR alpha in energy metabolism and vascular homeostasis. J. Clin. Invest. *116*, 571–580.

Leone, T.C., Weinheimer, C.J., and Kelly, D.P. (1999). A critical role for the peroxisome proliferator-activated receptor alpha (PPARalpha) in the cellular fasting response: the PPARalpha-null mouse as a model of fatty acid oxidation disorders. Proc. Natl. Acad. Sci. USA *96*, 7473–7478.

Li, J., Pircher, P.C., Schulman, I.G., and Westin, S.K. (2005). Regulation of complement C3 expression by the bile acid receptor FXR. J. Biol. Chem. *280*, 7427–7434.

Miyake, J.H., Doung, X.D., Strauss, W., Moore, G.L., Castellani, L.W., Curtiss, L.K., Taylor, J.M., and Davis, R.A. (2001). Increased production of apolipoprotein B-containing lipoproteins in the absence of hyperlipidemia in transgenic mice expressing cholesterol 7alpha-hydroxylase. J. Biol. Chem. *276*, 23304–23311.

Moreau-Hamsany, C., Castex, C., Hoo-Paris, R., Kacemi, N., and Sutter, B. (1988). Hormonal control of lipolysis from the white adipose tissue of hibernating jerboa (Jaculus orientalis). Comp. Biochem. Physiol. A *91*, 665–669.

Plotnikov, A.N., Hubbard, S.R., Schlessinger, J., and Mohammadi, M. (2000). Crystal structures of two FGF-FGFR complexes reveal the determinants of ligand-receptor specificity. Cell *101*, 413–424.

Rauch, J.C., and Behrisch, H.W. (1981). Ketone bodies: a source of energy during hibernation. Can. J. Zool. *59*, 754–760.

Rodriguez, J.C., Gil-Gomez, G., Hegardt, F.G., and Haro, D. (1994). Peroxisome proliferator-activated receptor mediates induction of the mitochondrial 3-hydroxy-3-methylglutaryl-CoA synthase gene by fatty acids. J. Biol. Chem. *269*, 18767–18772.

Scholz, R., Schwabe, U., and Soboll, S. (1984). Influence of fatty acids on energy metabolism. 1. Stimulation of oxygen consumption, ketogenesis and CO2 production following addition of octanoate and oleate in perfused rat liver. Eur. J. Biochem. *141*, 223–230.

Shimano, H., Horton, J.D., Hammer, R.E., Shimomura, I., Brown, M.S., and Goldstein, J.L. (1996). Overproduction of cholesterol and fatty acids causes massive liver enlargement in transgenic mice expressing truncated SREBP-1a. J. Clin. Invest. *98*, 1575–1584.

Simonet, W.S., Bucay, N., Lauer, S.J., and Taylor, J.M. (1993). A far-downstream hepatocyte-specific control region directs expression of the linked human apolipoprotein E and C-I genes in transgenic mice. J. Biol. Chem. *268*, 8221–8229.

Student, A.K., Hsu, R.Y., and Lane, M.D. (1980). Induction of fatty acid synthetase synthesis in differentiating 3T3-L1 preadipocytes. J. Biol. Chem. *255*, 4745–4750.

Tsuchida, A., Yamauchi, T., Takekawa, S., Hada, Y., Ito, Y., Maki, T., and Kadowaki, T. (2005). Peroxisome proliferator-activated receptor (PPAR)alpha activation increases adiponectin receptors and reduces obesity-related inflammation in adipose tissue: comparison of activation of PPARalpha, PPARgamma, and their combination. Diabetes *54*, 3358–3370.

Tugwood, J.D., Issemann, I., Anderson, R.G., Bundell, K.R., McPheat, W.L., and Green, S. (1992). The mouse peroxisome proliferator activated receptor recognizes a response element in the 5′ flanking sequence of the rat acyl CoA oxidase gene. EMBO J. *11*, 433–439.

Winegar, D.A., Brown, P.J., Wilkison, W.O., Lewis, M.C., Ott, R.J., Tong, W.Q., Brown, H.R., Lehmann, J.M., Kliewer, S.A., Plunket, K.D., et al. (2001). Effects of fenofibrate on lipid parameters in obese rhesus monkeys. J. Lipid Res. *42*, 1543–1551.

Yu, X., and White, K.E. (2005). FGF23 and disorders of phosphate homeostasis. Cytokine Growth Factor Rev. *16*, 221–232.

Zhang, J., Kaasik, K., Blackburn, M.R., and Lee, C.C. (2006). Constant darkness is a circadian metabolic signal in mammals. Nature *439*, 340–343.